Performance Enhancement of Active Power Filter with Resonant and Fuzzy Controllers using Implicit Closed Loop Current Control

K. Naga Viswaja[1], Dr.P.Sujatha[2]

[1] *Student, Department of EEE, JNTU Anantapur, Andhra Pradesh, India*
[2] *Professor, Department of EEE, JNTU Anantapur, Andhra Pradesh, India*

Abstract - *The loads mostly that are connected to the power system network are the non-linear loads. These loads generate harmonic pollution. These harmonic current components do not represent useful active power due to the frequency mismatch with the grid voltage. To reduce this harmonic content, active power filters are connected with the load. Error minimization is achieved by two different methods, the direct control method and the indirect control method. Indirect current control technique has simpler structure and better harmonic treating effect than direct current control. The indirect control methods are easier to implement since only the input variables (currents and voltages) are measured but the direct methods require highly complex reference generation mechanisms. In this paper Novel simple indirect control concepts for an active power filter (APF) with resonant controller and fuzzy controller are discussed. The main advantage over other control strategies is the achieved excellent simplicity-to-performance ratio. The proposed control strategies are based on the concept of virtual impedance emulation to provide high power factor in a system. The simulation results of Active Power Filter Control Strategy With Resonant Controller and fuzzy controller using Implicit Closed-Loop Current Control will be simulated in SIMULINK/ MATLAB environment to verify all deductions.*

Key words: Active Power Filter (APF), Control techniques, sensorless control strategies, fuzzy control.

1. INTRODUCTION

Nonlinear loads connected to the power system network generate harmonic pollution. Harmonic currents circulation through feeders and protective network elements produces energy losses that might interfere with other devices which are connected to the distribution network. Several other harmful effects are observed as presented in [1]. This problem becomes more intense with the increasing amount of electronic equipment. This equipment, a nonlinear load, is a source of current harmonics, which produce power losses and increase of reactive power in transmission lines. They have negative influence on the control and protection systems, and other electrical loads, resulting in reduced reliability. Reduction of harmonic content in line current to a few percent allows avoiding most of the problems. A remedy to the harmonic current injection problem is to connect passive, active [2], or hybrid filters in parallel with the loads.

Over the last few years, active power filters (APFs) have drawn great attention and are expected to be a suitable remedy for the problem. Two main categories of APFs exist: shunt filters and series filters. The shunt filters are effective for those nonlinear loads, which can be considered as current harmonic sources. Shunt filters are therefore used to generate harmonic currents to compensate load harmonic currents. Series filters are effective to generate harmonic voltages to compensate load harmonic voltages. In this paper shunt active power filters (APFs) are used [3]. APFs are the circuits which are based on switched power semiconductors that inject opposite phase harmonic currents at the point of common coupling (PCC). This results in the whole nonlinear load and APF system matching a nearly resistive load behavior at the PCC terminals.

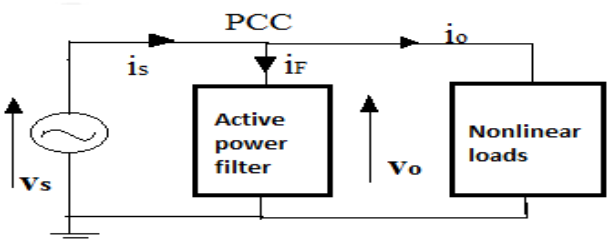

Fig 1: APF connected in parallel with the loads.

Power transmission in the network is made efficient, and all nonlinear load low-frequency-harmonic electromagnetic compatibility issues are reduced. Two tasks are crucial for an APF to perform well its function. They are the generation of appropriate current references and the ability to rapidly follow the reference current signals. Thus, shunt APFs use the error signal generated by the comparison of measured currents with the references. Minimizing such error is the main control

objective. Modulation signals to the inverter power section are generated by the employed controllers. This error can be minimized by two methods they are direct control method and indirect control method. In this project indirect control method is considered as these methods generate the APF current reference indirectly, i.e., by combining the currents of APF and nonlinear-load follow sinusoidal reference current signals in phase with the PCC voltages.

Therefore, using the scheme shown in Fig 1

$$i_F^* = i_s^* - i_o = i_{s,nonactive}^* - \sum_{h=1}^{N_h,max} i_{o(h)} \quad (1)$$

Where i_F^* and i_s^* are the APF and the PCC reference currents, respectively, $i_{s,nonactive}^*$ is the non active current component of the mains current *is*, and $i_{o(h)}$ represents the load-side current harmonics of order *h*. Even if the mains voltage presents harmonic distortion, this condition ensures that the correct inverter compensation current will be injected.

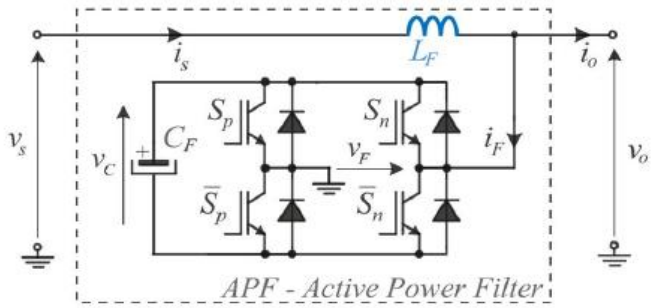

Fig 2: APF architecture used in this work.

Fig.2 shows the active power filter system architecture considered here [4]. The smoothing inductor *LF* is placed in series with the network and not with the voltage source inverter. The disadvantages of this architecture are that the inductor carries the full load current, except the harmonics, the PCC voltage *vo* is now switched, and due to load current harmonic components the load voltage can be distorted. Another aspect is that the rate of change of the load current is limited by the presence of *LF*. However, this APF structure implies an advantage from the APF control strategy point. Now the inductor current reference is sinusoidal and in phase with the mains voltage as is the APF modulating signal *m*(*t*). Therefore, the inductor current becomes independent from the harmonic currents of the load. It implies that

$$\overline{v_0} = \overline{v_F} = \hat{V}.\sin(\omega_1.t + \varphi) \quad (2)$$

Where x^- represents the local average value of *x* during a carrier period, $\hat{V}$ is the peak value of the mains voltage and $\omega 1$ is the mains voltage angular frequency. The proposed control strategy is much simpler to implement.

2. CURRENT CONTROL TECHNIQUES

There are two types of current control techniques they are direct current control technique and indirect current control technique. The difference between these two types of current control technique is in the number of current sensors used. For both the schemes a simple PI-controller is used to obtain reference current templates. Active power filter using indirect current control technique did not need compensation current measurement, but only detection devices for power supply voltage, power supply current and DC voltage. Compared with direct current control technique the indirect current controlled active power filter has simpler system structure and better harmonic treating performances. Therefore, such technique can effectively reduce system requirement for the hardware environment and is easy to implement with DSP technique.

A multiresonant controller is made of a set of resonant controllers, each tuned at a specific resonant frequency. The inverter is controlled by a multiresonant current controller. Resonant controller would be a good alternative, if it can satisfy the dual functions of regulation and selectivity. For the first function of current regulation, the resonant controller is sufficient to fulfill the task. The basic functionality of the PR controller is to introduce an infinite gain at a selected resonant frequency for eliminating steady state error at that frequency, and is therefore conceptually similar to an integrator whose infinite DC gain forces the DC steady-state error to zero. PR controllers have excellent current regulation performance for selected harmonics because large gain is assured for the resonant frequency. With the introduced flexibility of tuning the resonant frequency, attempts at using multiple PR controllers[5] for selectively compensating low-order harmonics. Another advantage associated with the PR controllers and filters is the possibility of implementing selective harmonic compensation without requiring excessive computational resources. With regard that selectivity is the most significant feature of controller.

A closed loop current control technique is used to reduce harmonics and the voltage regulations are carried out by PI controller. A current control loop is used to maintain the load current at some desired level. It requires the feedback currents from each phase. For current control the actual phase currents are compared with reference phase currents and the error is given to

PWM current controller to produce the switching signals for the inverter switches or it can be fed to a PI controller, to reduce it to an acceptable value. Now it is compared with a triangular carrier to produce the PWM signals. The design of filter inductance f_L is based on the current control technique used for generation of the switching pulse for the converter switches. In this work, carrier phase shifted PWM technique is used, in which two triangular signals will be compared with the generated reference signal. Total harmonic distortion has been improved. The important thing in APF is to maintain the capacitor voltage as constant [6]. For this, the capacitor voltage will be compared with a reference voltage and error signal will be processed through a PI controller through which capacitor voltage can be made constant.

3. CONTROL STRATEGY CONCEPTS

The interesting reduction technique of current harmonic is PWM rectifier. The PWM rectifier provides DC bus voltage stabilization and also acts as active line conditioner(ALC) that compensate harmonics and reactive power at the PCC. Reducing the cost of the PWM rectifier is important. The cost of power switching devices (e.g. IGBT) and digital signal processors (DSP.s) are decreasing and further reduction can be obtained by reducing the number of sensors. The sensorless methods[7] provides advantages to the system as: simplification, improved reliability and lower installation costs.

3.1 Current Sensorless Strategy

In current sensorless strategy reduction of current sensors is carried out. In AC current sensorless the solution is based on inductor voltage measurement in two lines. Supply voltage can be estimated with assumption that voltage on inductance is equal to line voltage. Applying Kirchhoff's second law to the circuit in Fig. 2 gives

$$v_S - L_F.\frac{di_S}{dt} - (s_p - s_n).v_c = 0 \qquad (3)$$

Where s_p and s_n are the switching functions for switches *Sp* and *Sn*, respectively. These are defined as +1 if a switch is closed and 0 when it is open. The resulting switching function for the filter comprehends both of these into$(s_p - s_n) = s_F$. The switching signals are generated by phase-shifted pulse width modulation. The high-frequency (HF) harmonics are typically eliminated with filters, and the following analysis considers only the low-frequency behavior of the circuit. This is achieved with the definition of the local average value $\bar{x}$ of the quantities within a switching period *Ts*. Applying this definition to the APF switching function leads to

$$\bar{S}_F = \frac{1}{T_S}\int_{t-T_S}^{t} S_F \; dt = d_F \qquad (4)$$

where d_F is the resulting APF duty cycle. This has to be generated by the control strategy. The result obtained when (4) is applied to (3) is

$$\bar{v}_S - L_F.\frac{d\bar{i}_S}{dt} - d_F\bar{v}_c = 0 \quad (5)$$

Assuming that a unity input power factor is to be achieved, the system should emulate a nearly resistive behavior. Thus

$$\bar{i}_s = \frac{\bar{v}_s}{R_e^*} \qquad (6)$$

Where R_e^* is the desired resistance value. The APF dc-link voltage is controlled with a variable *vm. This is* defined as

$$v_m = k\frac{V_c^*}{R_e^*} \quad (7)$$

Where *k* is the gain and V_c^* is the dc-link voltage reference. Isolating R_e^* in (7) and using it in (5) gives

$$\bar{v}_S - L_F.\frac{d}{dt}\left(\frac{\bar{v}_S v_m}{k V_c^*}\right) - d_F\bar{v}_c = 0 \quad (8)$$

Assuming a purely sinusoidal $\bar{v}_S$ leads to

$$\frac{d}{dt}(\bar{v}_s) = -\omega^2 \int \bar{v}_s \, dt \quad (9)$$

where ω is the sine angular frequency. The control signal v_m is assumed constant at steady state. Thus, (8) is rewritten as

$$\bar{v}_S + \frac{\omega^2 L_F}{k V_c^*}\int(\bar{v}_s v_m)dt - d_F\bar{v}_c = 0 \quad (10)$$

Defining

$$k_1 = \frac{\omega^2 L_F}{k V_c^*} \quad (11)$$

and replacing it in (9) results in

$$d_F = \frac{\bar{v}_s}{v_c} + \frac{k_1}{v_c}\int(\bar{v}_s v_m)dt \quad (12)$$

The resulting control block diagram is shown in Fig.3. This control strategy is simple and does not require complex computations for the generation of references. The phase-shifted PWM leads to the output of the inverter generating a voltage with twice the carrier

frequency and with reduced current ripple. The procedure to determine the duty cycle described earlier is input current sensorless and has the advantage of only measuring the input and the dc-link voltages to generate the control signal.

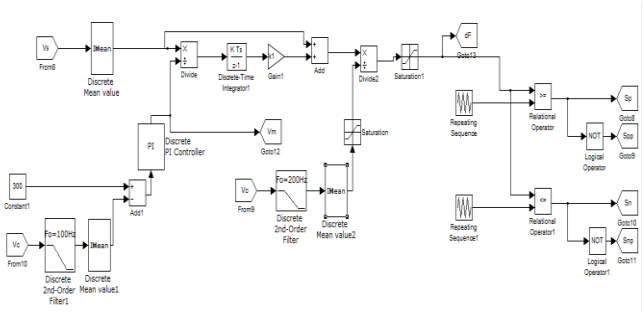

Fig.3: Block diagram for the current sensorless control strategy based on equation (12)

3.2 Voltage Sensorless Strategy

Similar to input current sensorless strategy, an input voltage sensorless strategy is derived in the following. The dc current control should work effectively when the reference value of the dc current is changed. For that reason, a non-linear PI controller, where the input of the controller is the square of the error signal, is proposed for the control systems. With small error values the controller acts slowly and when the error value is increased faster control dynamics is achieved.

Replacing *vs* from (6) in (5) gives

$$R_s^* \bar{i}_s - L_F \cdot \frac{d\bar{i}_s}{dt} - d_F \bar{v}_c = 0 \quad (13)$$

During sinusoidal steady state

$$\frac{d}{dt}(\bar{i}_s) = -\omega^2 \int \bar{i}_s \, dt \quad (14)$$

Defining the dc-link voltage control signal as

$$v_m = \frac{R_s V_c^*}{R_s^*} \quad (15)$$

Where *Rs* is the current measurement gain, and substituting the before mentioned relations into (13) lead to

$$V_c^* R_s \frac{r_s}{v_m} + \omega^2 L_F \int \bar{i}_s \, dt - d_F \bar{v}_c = 0 \quad (16)$$

Defining gain k_2 as

$$k_2 = \frac{L_F \omega^2}{R_s V_c^*} \quad (17)$$

and dividing (16) by *Vc* Rs* finally gives the duty cycle

$$\frac{d_F}{R_s V_c^*} = \frac{r_s}{v_m v_c} + \frac{k_2}{v_c} \int \bar{i}_s \, dt \quad (18)$$

The voltage sensorless control strategy [8] based on (18) is implemented with the block diagram shown in Fig. 4.

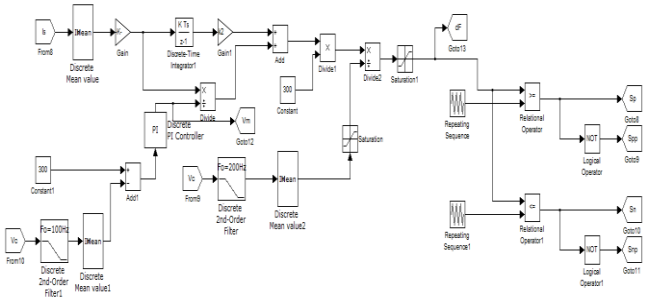

Fig.4: Block diagram for the voltage sensorless control based on equation (18).

The strategy is straightforward and similar from the practical implementation aspects to the current sensorless one. The advantage of this approach over the current sensorless one is that over current protection techniques are easier to implement with the current measurement.

4. FUZZY LOGIC

In recent years, the number of applications of fuzzy logic has increased significantly. The applications range from consumer products such as cameras, camcorders, washing machines, and microwave ovens to industrial process control and medical instrumentation. Fuzzy logic (FL) is almost synonymous with the theory of fuzzy sets, a theory which relates to classes of objects with unsharp boundaries in which membership is a matter of degree. The basic concept underlying FL is that of a linguistic variable, that is, a variable whose values are words rather than numbers. In effect, much of FL may be viewed as a methodology for computing with words. Although words are inherently less precise than numbers, they can be understood immediately and easily. Another basic concept in FL, which plays a major role in most of its applications, is that of a fuzzy if-then rule or, simply, fuzzy rule. Although rule-based systems have a long history of use in Artificial Intelligence (AI), what is missing in such systems is the mechanism for dealing with fuzzy consequents and fuzzy antecedents. In fuzzy logic, this mechanism was provided by the calculus of fuzzy rules. The fuzzy logic toolbox is highly impressive in all respects. It makes fuzzy logic an

effective tool for the conception and design of intelligent systems. The fuzzy logic toolbox is easy to implement and convenient to use. It provides a reader friendly and up-to-date introduction to methodology of fuzzy logic and its wide ranging applications.

4.1 Fuzzy Logic Controllers

The word Fuzzy means vagueness. Fuzziness occurs when the boundary of piece of information is not clear-cut. In 1965 Lotfi A.Zahed propounded the fuzzy set theory. Fuzzy set theory exhibits great potential for effective solving of the uncertainty in the problem. Fuzzy set theory is an excellent mathematical tool to handle the uncertainty arising due to vagueness. Understanding human speech and recognizing handwritten characters are some common instances where fuzziness manifests. Fuzzy set theory is an extension of classical set theory where elements have varying degrees of membership. In FLC the input variables are mapped by sets of membership functions and these are called as "FUZZY SETS". Fig.5 shows basic FUZZY module.

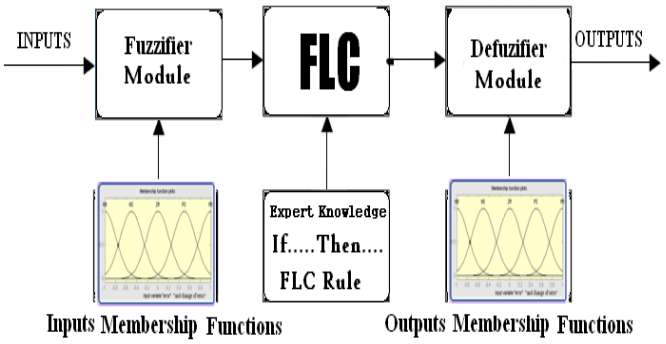

Fig.5: Fuzzy Basic Module

e/de	NB	NM	NS	Z	PS	PM	PB
NB	NB	NB	NB	NB	NB	NB	NB
NM	NB	NM	NM	NM	NS	NS	NS
NS	NB	NM	NM	NS	NS	NS	Z
Z	Z	Z	Z	Z	Z	Z	Z
PS	Z	PS	PS	PS	PM	PM	PB
PM	PS	PS	PS	PM	PM	PB	PB
PB	PB	PB	PB	PB	PB	PB	PB

Table 1: Control strategy based on 49 Fuzzy control Rules with combination of seven error states multiplying with seven changes of error states.

Fuzzy set comprises from a membership function which could be defines by parameters. The value between 0 and 1 reveals a degree of membership to the fuzzy set. The process of converting the crisp input to a fuzzy value is called as "fuzzificaton [9]." The output of the Fuzzier module is interfaced with the rules. The basic operation of FLC is constructed from fuzzy control rules utilizing the values of fuzzy sets in general for the error and the change of error and control action. The results are combined to give a crisp output controlling the output variable and this process is called as the "DEFUZZIFICATION."

The PI controller in Fig.3 and Fig.4 are replaced with FUZZY controller and results are observed. The results are improved when fuzzy controller is connected. The THD values are reduced.

5. SIMULATION RESULTS

The power stage configuration used in the simulation-based analysis of the APF system is shown in Fig. 6. A low APF switching frequency of *fc* = 5 kHz is used to highlight the performance of the proposed concepts. The nonlinear load is a single-phase diode bridge rectifier with the following parameters:
Ro = 40 Ω, *Co* = 940 μF, L_2 = 1 mH.

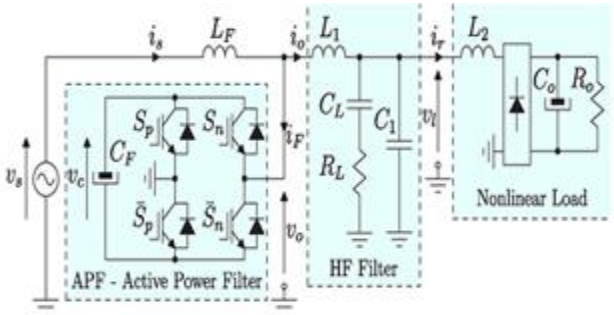

Fig.6: APF power stage setup used in the simulation results

Other experimental parameters are as follows:
Input ac voltage is set to *Vs*,rms = 110 V,
Main frequency *fs* = 60 Hz,
APF inductance *LF* = 12.83 mF,
HF filter inductance *L*1 =1.4 mH,
HF filter resistance *RL* = 2 Ω,
HF filter capacitance *CL* = 8 μF, and
HF filter capacitance *C*1 = 0 μF

The simulation results are shown in Figs. (7) and (8) for the voltage sensorless control strategy with PI and in Figs. (12) and (13) with FUZZY controllers. The Mains current Is , APF control variable d_F and the Load voltage V_l are shown in Fig.(8) for PI controller and in Fig.(13) for FUZZY controller . The mains current i_s shown in Fig. 8, is in phase with the mains voltage despite the large filter inductance of L_F = 12.83 mH. Thus, it proves the capability of the novel APF concept to emulate a resistive behavior when observed from the mains. Finally, Fig .8, shows the APF duty cycle and the load voltage at the terminals of the C_L–R_L branch with the respective THD value of 9.65%. When PI controller is replaced with FUZZY controller the exact error percentage can be obtained and distortions can be reduced. The THD value of load voltage obtained with FUZZY controller is 4.81%

Similar results are found for the current sensorless control strategy as seen in the respective graphs shown in Figs.(9) and (10) with PI and in Figs,(14) and(15) with FUZZY controller . Fig. 10, shows the load voltage at the terminals of the $CL–RL$ branch with the respective THD value of 9.83%. It can be seen that harmonic distortion appears as the load current causes a distorted voltage across inductor $L1$, which is partially filtered with the parallel branch $RL–CL$. This effect should be analyzed on a case-based approach in order to evaluate the load voltage. Reducing inductor $L1$, increasing CL, and/or including capacitance $C1$ reduces the load voltage distortion. When PI controller is replaced with FUZZY controller the distortions can be reduced. The THD value of load voltage obtained with FUZZY controller is 4.86%

In order to compare the transient performances of the current sensorless control strategies, a simulation with the same conditions including an input voltage step at t = 1.1 s from 100% to 120% of rated voltage and a load step from 75% to 100% of rated power at t = 1.75 s was carried out. The result for the power factor variation during load change is shown in Fig. 11. As it is very difficult to observe the differences in the mains current, a variable related to the power factor is used. This local power factor variable is defined as

$$(\lambda)_{T_g} = \frac{\frac{1}{T_g}\int_{t-T_g}^{t} v_0 i_0 dt}{\sqrt{\frac{1}{T_g}\int_{t-T_g}^{t} v_s^2 dt}\sqrt{\frac{1}{T_g}\int_{t-T_g}^{t} i_s^2 dt}} \qquad (19)$$

Where T_g is the mains fundamental period. It gives the correct power factor at steady state and an impression of the power deviations during transients. Fig. 11, shows that the combined method gives shorter transients and that both methods achieve close-to-unity power factor at steady state for all tested load conditions. Both control strategies have presented similar results regarding the mains-side current is and the APF dc-link voltage vc, which are exemplarily shown in Fig. 11. The settling time was below 1 s for the given simulation conditions and is mainly dictated by the APF dc-link voltage control loop. The simulation results during an input voltage transient at t = 1.1 s from 100% to 120% of rated voltage and a load transient from 75% to 100% of rated power at t = 1.75s for the current sensorless control strategy with PI and FUZZY controllers are shown in Figs. (11) and (16). The THD value of i_s when PI controller is connected during load change is 3.09% and when FUZZY controller is connected is 1.56%.

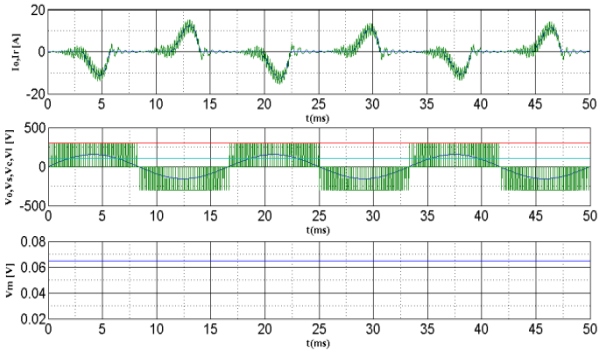

Fig 7: voltage sensorless control strategy with PI
a) Load-side PCC current *Io* and rectifier current I*r*.
(b) APF capacitor voltage *Vc*, APF output voltage *Vo*, and mains voltage *vs*. (c) DC link control variable *Vm*.

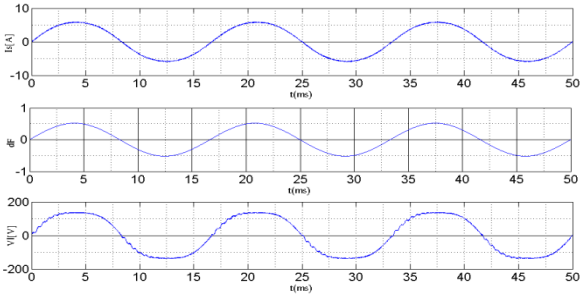

Fig 8: voltage sensorless control strategy with PI
(a) Mains current Is (b) APF control variable *dF*
(c) Load voltage Vl.

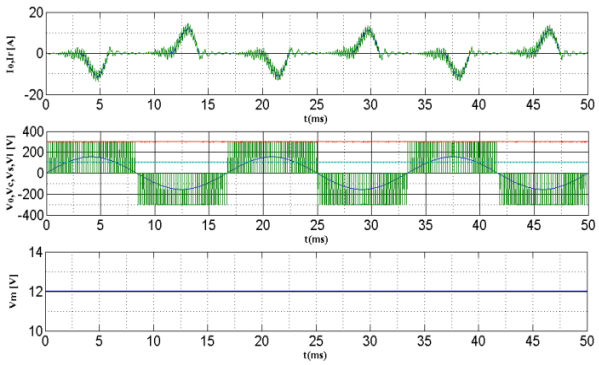

Fig 9: current sensorless control strategy with PI
a) Load-side PCC current *Io* and rectifier current *Ir*.
(b) APF capacitor voltage *Vc* APF output voltage *Vo*, and mains voltage Vs. (c) DC link control variable *Vm*.

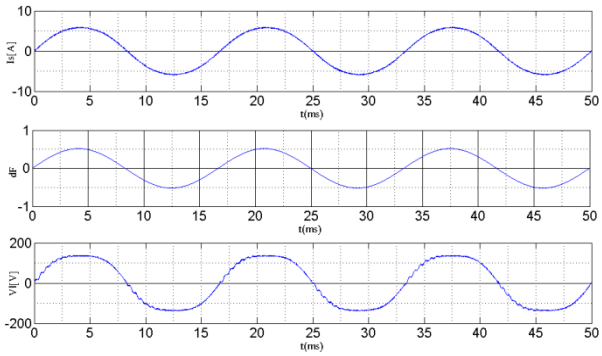

Fig 10: current sensorless control strategy with PI
(a) Mains current *is* (b) APF control variable *dF*
(c) Load voltage Vl.

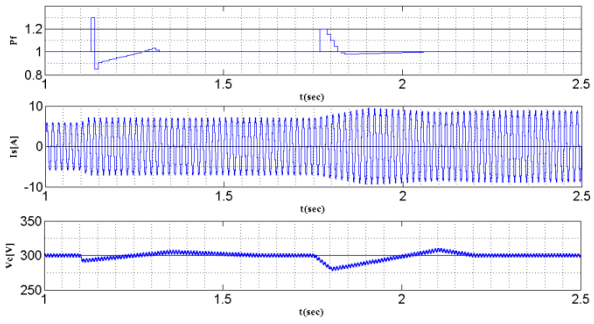

Fig.11: Simulation result waveforms for the current sensorless indirect control strategy with PI
(a) Local power factor value according to (19).
(b) Mains current *is*. (c) APF capacitor voltage V*c* during load change

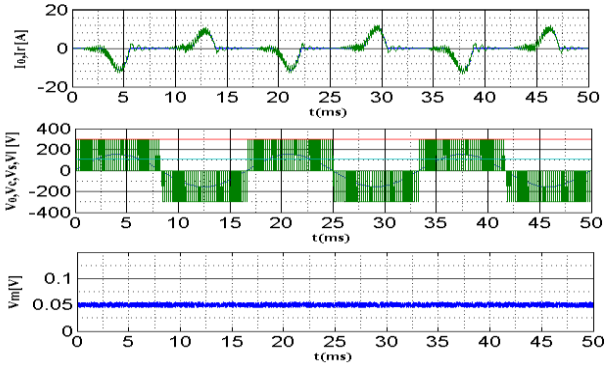

Fig 12: voltage sensorless control strategy with FUZZY
a) Load-side PCC current *Io* and rectifier current *Ir*.
(b) APF capacitor voltage *Vc*, APF output voltage V*o*, and mains voltage *vs*. (c) DC link control variable V*m*.

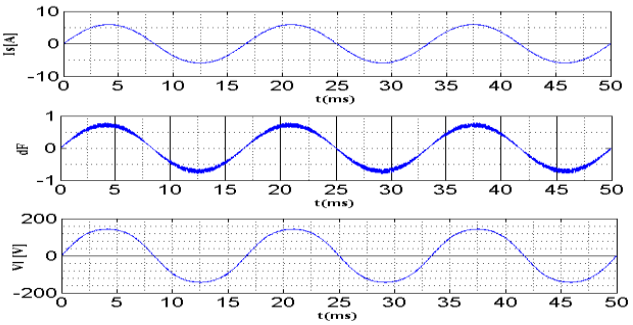

Fig 13: voltage sensorless control strategy with FUZZY
(a) Mains current *is* (b) APF control variable *dF*
(c) Load voltage Vl.

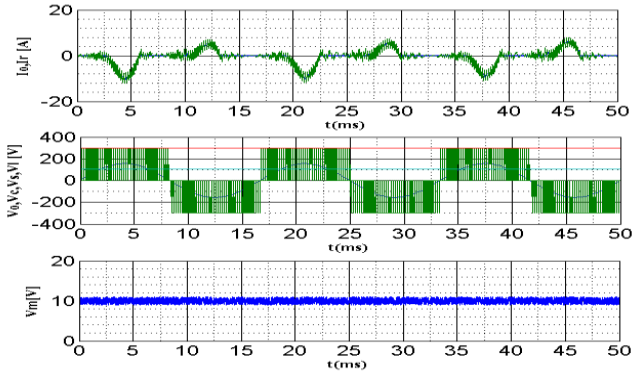

Fig 14: current sensorless control strategy with FUZZY
a) Load-side PCC current *Io* and rectifier current *Ir*.
(b) APF capacitor voltage *Vc*, APF output voltage *Vo*, and mains voltage *Vs*. (c) DC link control variable *Vm*.

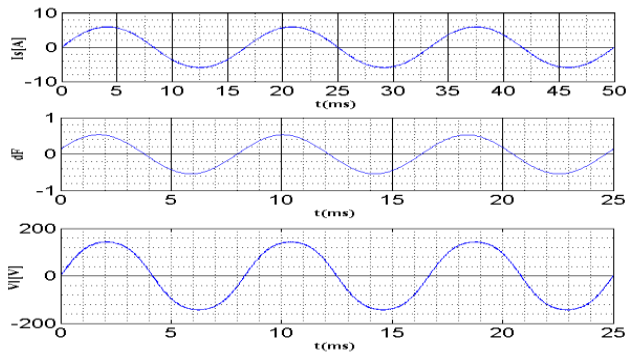

Fig 15: current sensorless control strategy with FUZZY (a) Mains current *Is* (b) APF control variable d_F (c) Load voltage V_l.

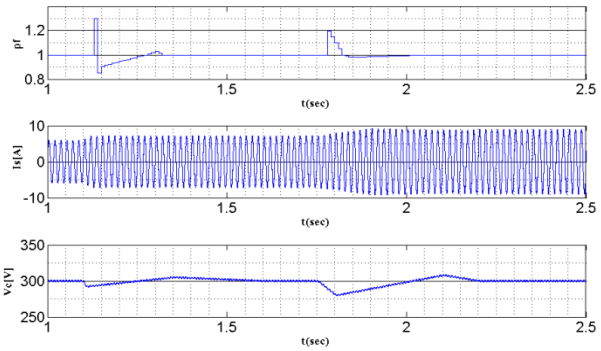

Fig.16: Simulation result waveforms for the current sensorless indirect control strategy with FUZZY (a) Local power factor value according to (19). (b) Mains current Is. (c) APF capacitor voltage *Vc* during load change

6. CONCLUSIONS

Control strategies for shunt APF architecture have been proposed here. The proposed strategies were able to guarantee close-to-unity power factor. Both current and voltage sensorless versions have been presented, where the current sensorless control has been analyzed in detail regarding its performance and equivalent circuits with PI and FUZZY controllers. The implicit control loop is another innovative characteristic. These characteristics were verified through circuit simulation including a nonlinear rectifier load. This is a very low switching and highlights the achievable performance. The THD values are reduced when FUZZY controller is connected compared with PI controller. The concepts can be easily extended to the control of PFC rectifiers and three –phase systems.

REFERENCES

[1] P. Salmeron and S. Litran, "Improvement of the electric power quality using series active and shunt passive filters," *IEEE Trans. Power Del.*, vol. 25, no. 2, pp. 1058–1067, Apr.2010.

[2] H. Akagi, A. Nabae, and S. Atoh, "Control strategy of active power filters using multiple voltage-source PWM converters," *IEEE Trans. Ind. Appl.*, vol. IA-22, no. 3, pp. 460–465,May1986.

[3] Y. Tang, P. C. Loh, P. Wang, F. H. Choo, F. Gao, and F. Blaabjerg, "Generalized design of high performance shunt active power filter with output LCL filter," *IEEE Trans. Ind. Electron.*, vol. 59, no. 3, pp. 1443–1452, Mar. 2012.

[4] G.-Y. Jeong, T.-J. Park, and B.-H. Kwon, "Line-voltage-sensorless ac tive power filter for reactive power compensation," *Proc. Inst. Elect. Eng.—Elect. Power Appl.*, vol. 147, no. 5, pp. 385–390, Sep. 2000.

[5].R. Teodorescu, F. Blaabjerg, M. Liserre, and P. C. Loh, "Proportional resonant controllers and filters for grid-connected voltage-source converters,"*Proc. Inst. Elect. Eng.—Elect. Power Appl.*, vol. 153, no. 5, pp. 750–762, Sep. 2006.

[6] A. Bhattacharya and C. Chakraborty, "A shunt active power filter with enhanced performance using ANN-based predictive and adaptive controllers,"*IEEE Trans. Ind. Electron.*, vol. 58, no. 2, pp. 421–428,Feb. 2011.

[7] M. Salo, "AC current sensorless control of the current-source active power filter," in *Proc. IEEE 36th PESC*, Jun. 2005, pp. 2603–2608.

[8] Mauricio Angulo, Domingo A. Ruiz-Caballero, "Active Power Filter Control Strategy With Implicit Closed-Loop Current Control and Resonant Controller" *IEEE transactions on ind. Electron.*, vol. 60, no. 7,pp. 2721-2730, july. 2013

[9]. K. Passino and S. Yurkovich, Fuzzy Control,CA: Addison-Wesley Longman,Inc.1998.

BIOGRAPHIES

K. Naga Viswaja currently pursuing M.Tech in Electrical Power Systems at JNTUA College of Engineering and Technology Anantapur, Andhra Pradesh. Her area of interest is Power Systems.

Dr.P. Sujatha is a Professor and Head of the department of Electrical Engineering at JNTUA College of Engineering and Technology, Anantapur, Andhra Pradesh. Her areas of interest are Electrical Power Systems and Energy Management.

